

# Evaluation of TAERO UGV structural collision resistance using FEM analysis

Marek NOWAKOWSKI<sup>✉\*</sup> and Krzysztof KOSIUCZENKO<sup>✉</sup>

Military Institute of Armoured and Automotive Technology, Okuniewska 1, 05-070 Sulejów, Poland

**Abstract.** The increasing adoption of unmanned platforms in sectors such as defense, agriculture, and logistics highlights critical challenges, including traversal capability and collision resistance in unstructured terrain. This study investigates the crashworthiness of the developed TAERO UGV using finite element method (FEM) analysis. The structural components critical to collision energy absorption were identified and analyzed. Descriptions of the LS-DYNA simulation model, material properties, and boundary conditions are provided. The primary objective was to numerically assess the bumper performance during impact, considering the operational speeds and crumple zone of the vehicle. An optimized numerical model was introduced to efficiently simulate vehicle collisions, focusing on key structural elements. Various scenarios were simulated to examine deformation, stress distribution, and bumper behaviour. Presented numerical analysis indicates that impacts with typical obstacles, like tree trunks in unstructured terrain, cause minimal damage, not affecting the operational vehicle capability. Minor bumper damage, such as dents, vary and are more noticeable at higher speeds, while almost imperceptible up to 25 km/h. Stress distribution highlights the role of side components in energy absorption and structural deformation. The results confirm the structural integrity of the vehicle and provide valuable data on its operation performance in complex environments during specialized missions.

**Keywords:** UGV; structural collision resistance; crumple zone; FEM analysis.

## 1. INTRODUCTION

The use of unmanned ground vehicles (UGVs) has grown significantly in recent years, driven by their ability to perform diverse tasks in hazardous and challenging environments. These unmanned platforms provide precise operation and reduce risks to human operators through remote or autonomous modes, making them valuable in both commercial and civilian applications [1]. In military applications, UGVs are used in high-risk missions, such as reconnaissance, explosive ordnance disposal, and resupply in combat zones [2]. Unmanned platforms are mainly deployed in off-road terrains characterized by dense vegetation and unstructured terrain [3]. Their roles include complex operations, like evacuating casualties under fire and navigating areas contaminated with hazardous substances across landscapes challenged by obstacles such as roots, trees, underbrush, and rugged ground [4]. Despite the absence of humans on board, the structural durability of UGVs remains a crucial design consideration. Sensitive equipment like sensors and communication systems require the vehicle frame and critical components to withstand impacts [5]. In teleoperated mode, limited situational awareness and challenging visibility make collision avoidance difficult. Autonomous systems, despite their advanced capabilities, still face challenges in detecting obstacles in real time increasing the risk of unintended collisions with natural barriers highlighting the need for robust structural collision resistance. Damage to the vehicle structure can result in the loss of high-value technology and negatively impact the success of critical missions.

Therefore, unmanned platforms must be designed to withstand impacts without compromising functionality or mission success, making crash resistance assessment essential for ensuring operational reliability and long-term durability [6]. Key factors such as frame integrity, component connections [7,8], material properties [9], and the potential for additive manufacturing replacements [10] all influence the vehicle ability to respond to collisions.

To address these challenges, simulation-based methods have been increasingly adopted as cost-effective alternatives to real-world testing, which is both expensive and time-consuming. In recent studies [11] authors utilized SolidWorks simulation software to analyze the chassis of a UGV, focusing on stress distribution and deformation under extreme conditions. Their work highlighted the importance of accurate mesh modelling in FEM, which is crucial for obtaining reliable results regarding the strength of the UGV chassis. Moreover, a structural optimization study of a UGV frame was conducted using response surface analysis (RSA) and topology optimization (TO) [12]. This approach not only identifies critical load cases but also improves the load-carrying capacity of the unmanned platform structure. The integration of FEM with optimization techniques provides a framework for improving the crashworthiness of UGVs, ensuring they can withstand impacts while maintaining operational functionality. In addition to structural analysis, understanding the dynamics of UGVs during collision scenarios is also critical for evaluating crash performance [13].

The study evaluates the structural collision resistance of the TAERO UGV using finite element method analysis, focusing on typical obstacles in operational environments. The analysis examines stress distribution, deformation, and energy absorption to identify operational conditions the UGV can traverse.

\*e-mail: Marek.Nowakowski@witpis.eu

Manuscript submitted 2024-11-27, revised 2025-01-08, initially accepted for publication 2025-01-27, published in May 2025.

## 2. DESCRIPTION OF TAERO VEHICLE AND OPERATIONAL CONDITIONS

TAERO is a manned-unmanned platform developed by the consortium: Military Institute of Armoured and Automotive Technology (WITPiS), Stekop, Auto Podlasie, and AP Solutions. Built on a modular design, TAERO (Fig. 1) is highly adaptable and can be customized for a wide range of missions in both military and civilian applications [14]. This modular architecture facilitates the integration of various specialized modules, such as optoelectronic head, weapons, and threat detection technologies, allowing TAERO to meet the diverse needs of its users.



(a)



(b)

**Fig. 1.** View of TAERO vehicle in configurations: manned (a) and unmanned (b)

TAERO is equipped with advanced technology to support its operations. A central processing unit manages the data from various sensors and systems. The vehicle uses a precise GPS integrated with an inertial measurement unit (IMU) for accurate navigation, ensuring reliable positioning even in challenging environments. Additionally, situational awareness sensors are used to detect obstacles, while mechatronic drives are employed to manage vehicle movement. These systems work together to ensure that TAERO can perform tasks such as navigating rough terrain, avoiding obstacles, and making real-time decisions.

In unmanned mode, TAERO can perform a range of operations. These include teleoperation, autonomous navigation along predefined routes, following a guide vehicle, or conducting missions in silent mode, which is powered by its electric drive. This flexibility makes TAERO an essential tool for operations where traditional vehicles cannot be used or where human risk must be

minimized. These diverse conditions introduce significant challenges that go beyond the capabilities of manned vehicles. One of the most challenging operational scenarios for UGVs occurs in unstructured environments, where obstacles such as vegetation, rocks, and hidden hazards can severely impact terrain traversability (Fig. 2).



**Fig. 2.** Examples of operational conditions in unstructured terrain

Vegetation increases the risk of navigation failures, unexpected stops, or even vehicle damage. Therefore, UGVs like TAERO need to analyze basic resistance to common obstacles, such as tree trunks, to ensure continued operation and prevent mission disruptions.

## 3. NUMERICAL MODELLING OF TAERO VEHICLE STRUCTURE

### 3.1. Defining crumple zone

Numerical modelling of the TAERO structure is crucial for evaluating its collision resistance and mechanical performance under various operational scenarios. To ensure safe operation and prevent circumstances that could immobilize the vehicle during a collision, a crumple zone was defined as a key design element. This zone is considered a critical feature, designed to absorb impact energy and minimize the forces transmitted to the passenger compartment and essential systems, such as the engine, radiator, and fuel components.

The TAERO vehicle, designed for demanding off-road applications, required a unique approach to optimize the layout of its front-end components. Unlike conventional vehicles, which rely on plastic energy absorbers that can easily be damaged in unstructured environments [15], the TAERO structure utilizes high-strength materials, such as reinforced bumpers and side members, for greater durability.

Due to its specialized purpose, the crumple zone was expanded, and critical components were strategically positioned to maximize energy dispersion. Key elements, such as the engine, control units, and battery, were placed away from high impact areas to minimize the risk of damage. The vehicle was designed for deployment via airdrop on the PDS platform and for transportation as a sling load under a helicopter, requiring an exceptionally durable frame. This design approach ensures the

## Evaluation of TAERO UGV structural collision resistance using FEM analysis

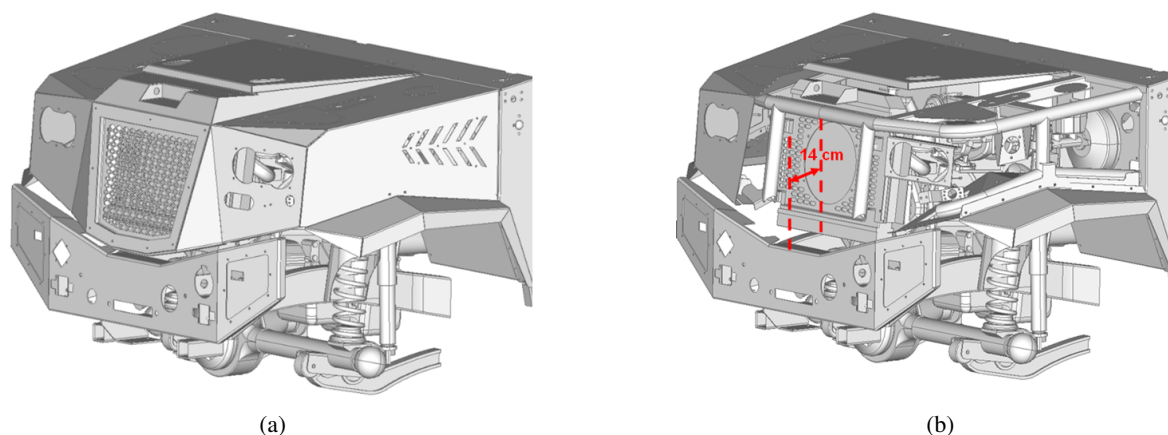


**Fig. 3.** View of front structure of TAERO vehicle (a) and determination of the crumple zone (b) as the distance between the bumper and the radiator

distribution of impact forces over a larger area, enhancing both safety and operational reliability.

The crumple zone was engineered to deform progressively, with different sections absorbing energy at varying rates. Based on the available 3D model, the depth of the crumple zone was determined to be  $L = 14$  cm as shown in Fig. 3.

This controlled deformation helps distribute impact forces over time, optimizing energy dissipation and reducing stress on the critical components.

### 3.2. TAERO vehicle model for computational purpose

In general, simulating the collision behaviour between a vehicle and an obstacle is complex, as it involves the interaction of numerous structural components. Accurately modelling this process can be highly time-consuming and requires computational resources, which may not always be in line with the accuracy gained.

Considering the aforementioned, a simplified physical model of the TAERO vehicle was developed for numerical analysis in the LS-DYNA environment [16]. In this model, only the structural elements with the most noteworthy influence on collision behaviour, such as the bumper and the main vehicle frame consisting of side and cross-connections, were modelled. All other structural components were combined into a single equivalent mass element (MASS), positioned at the vehicle centre of mass (with a total mass of 2800 kg), to ensure accurate inertial properties as shown in Fig. 4a. The MASS element was connected to the frame with RBE2 (Rigid Body Element, Form 2) as shown in Fig. 4b.

The obstacle was modelled as a wooden trunk fixed firmly to the ground. The strong root system of pine trees was simulated by securing the obstacle to the ground with a fixed node-to-node connection to reflect realistic ground attachment. All components with mass were subjected to gravitational acceleration  $g = 9.81 \text{ m/s}^2$ , and a velocity vector ( $v$ ) was assigned, varying according to the different simulation scenarios. The velocity vector should be understood as the initial speed at the moment of the collision onset. Due to the small duration of the phenomena,

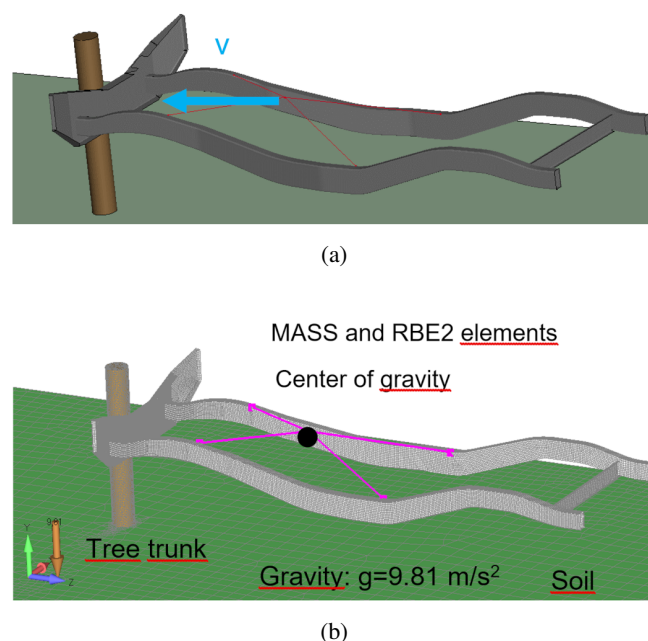


**Fig. 4.** The model of TAERO vehicle (a) including mass equivalent and obstacle used for computational purpose and related mesh structure (b)

gravity does not significantly affect the calculation results and the vertical displacement of the frame, nevertheless, all degrees of freedom were blocked at the centre of gravity of the frame, except for the displacement along the vehicle.

For the simulation, a trunk diameter of 15 cm was chosen, representing an average value for mature pine trees in these forests. This assumption is supported by published data indicating that Scots pine covers approximately 58% of the tree stand in Poland, making it the dominant forest-forming species in the country [17]. This value aligns with observations made during the recent Field Experimentation Exercise (FEX 2024) in Poland, where the TAERO vehicle was tested in a similar environment. Furthermore, other prevalent species such as spruce and oak exhibit comparable trunk diameters within this age



range, further reinforcing the validity of the selected diameter for this study.

The geometry of the physical model was represented using a finite element mesh (Fig. 4b). For the vehicle structural elements and the ground, flat 4-node SHELL elements (with a size of 2–10 mm) were used, with a thickness of 3 mm. In contrast, the obstacle was modelled with three-dimensional SOLID elements to capture the interaction and deformation more accurately during impact.

To improve the accuracy of the collision simulation, the mesh density was increased at the contact point between the bumper and the obstacle. A density ratio of 4:1 was applied in this region to provide a finer resolution for more precise calculations of the forces and deformations involved (Fig. 5).

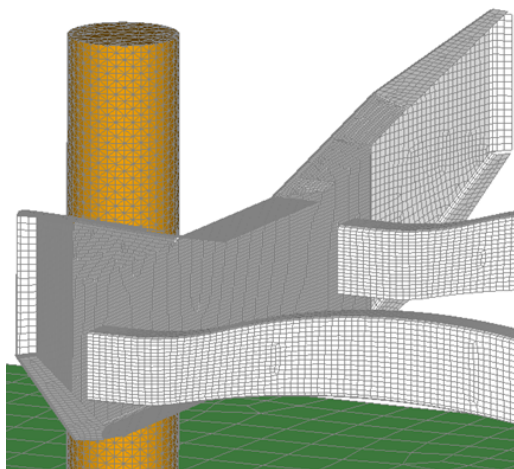


Fig. 5. Applied dense mesh for improved accuracy

### 3.3. Material properties used in software environment

Modelling wooden parts for numerical purposes presents significant challenges due to their anisotropic properties. LS-DYNA provides several material models designed to simulate wood behaviour, with the most commonly used being MAT\_143 (Wood), MAT\_181 (simplified rubber/foam), and MAT\_163 (modified crushable foam) [16]. In this study, the MAT\_143 model was selected due to its ability to accurately represent the orthotropic nature of wood, which is essential for simulating its features in different directions.

The MAT\_143 model considers the nonlinear response of wood, including differences in behaviour under compression and tension, as well as the influence of moisture content. Additionally, this model is capable of simulating wood cracking and failure, offering significant flexibility in defining material parameters. This flexibility allows the model to be customized for various wood species.

For this simulation, the obstacle was modelled as a single tree trunk with a cross-sectional diameter of 15 cm. The material properties used for this simulation were as follows: wood density  $\rho = 500.0 \text{ kg/m}^3$ , Poisson's ratio  $\nu = 0.35$ , and the elastic modulus are specified as follows:

- EL (along the wood grain): 12 GPa;
- ET (across the wood grain): 400 MPa;

- GLT (longitudinal-transverse shear modulus): 750 MPa;
- GTR (radial-tangential shear modulus): 75 MPa.

The following strength of the tree trunk was assumed:

- XT (tension along the wood grain): 85 MPa;
- XC (compression along the wood grain): 41 MPa;
- YT (tension across the wood grain): 3 MPa;
- YC (compression across the wood grain): 5.5 MPa;
- SXY, SYZ (shear strength): 9 MPa.

In LS-DYNA simulations, two material models are commonly used for evaluating the crashworthiness of vehicle chassis made from structural steel, such as S235JR. One of the most widely used models is MAT\_PIECEWISE\_LINEAR\_PLASTICITY, which allows for the nonlinear behaviour of steel to be modelled by defining a stress-strain curve [16]. This model is relatively simple to implement and is often employed in quasi-static simulations.

A more advanced material model, MAT\_JOHNSON\_COOK, is preferred for collision test simulations due to its enhanced capabilities in modelling dynamic impacts [18]. This model accounts for the effects of strain rate and temperature on the material behaviour, making it particularly suitable for high-speed collisions. The MAT\_JOHNSON\_COOK model describes changes in yield strength as a function of plastic strain, strain rate, and temperature, providing a more comprehensive representation of steel behaviour under dynamic conditions.

Specifically, the model incorporates the influence of strain rate, which is crucial in fast impacts, as well as the material property changes due to heating during deformation. It allows for a more accurate prediction of plastic deformation and fracture, offering a better representation of steel behaviour in dynamic scenarios. Given these capabilities, MAT\_JOHNSON\_COOK was selected for this work to ensure more accurate results in collision test simulations.

The following parameters were implemented in the model:

- A (yield strength): 280 MPa;
- B (hardening modulus): 490 MPa;
- n (hardening exponent): 0.31;
- C (strain rate sensitivity coefficient): 0.022;
- m (thermal softening exponent): 0.9;
- TM (melting temperature): 1800 K;
- TR (reference temperature): 293 K;
- EPSO (Reference strain rate ( $0.001 \text{ s}^{-1}$ ));
- CP (specific heat capacity): 452 J/(kg K).

The surface on which the TAERO vehicle was modelled as a  $10 \times 10 \text{ m}$  plane, represented by a mesh consisting of square SHELL-type finite elements. To improve computational efficiency, due to the absence of direct interaction with the vehicle structure, these elements were assigned RIGID material properties. The plane was connected to the obstacle at specific nodes.

The ground plane was fixed at its four corners using translational constraints, restricting movement in the X, Y, and Z directions (TX, TY, TZ). This ensured the stability and immobility of the ground surface throughout the simulation. To accurately simulate the vehicle motion dynamics, a constant velocity vector was applied to the MASS element representing the vehicle mass, with the value corresponding to the specific calculation scenario.

The vehicle interaction with the obstacle was defined by maintaining an initial distance of 7 cm between the vehicle and the obstacle surface. This distance was overcome in a time span of 2.5 to 7.5 ms, depending on the simulation conditions. This setup allows for precise modelling of the early collision phase, where the interaction between the vehicle and the obstacle plays a critical role.

Considering the expected damage and deformation of the vehicle structural components during impact, the contact type was defined as `ERODING_NODES_TO_SURFACE` [18]. This contact type enables the dynamic removal of nodes and elements from the model, a crucial feature in collision simulations where significant material failure is expected.

#### 4. RESULTS OF NUMERICAL CALCULATIONS

The simulations generated results including instantaneous stress, displacement, and strain maps, as well as visual representations of material failure, as shown in Fig. 6.

To improve the clarity of the analysis, additional components (grey), such as wheels, were incorporated into the model for

visualization purposes only. The results indicate that extreme stresses occur at the points of direct contact with the obstacle and at the locations where the frame connects to the bumper, highlighting their significant role in energy transfer and structural deformation during impact.

Numerical calculations were conducted using the LS-DYNA environment on the OKEANOS supercomputer at the ICM (Interdisciplinary Centre for Mathematical and Computational Modelling at the University of Warsaw). It is a high-performance Cray XC40 system designed to support complex scientific simulations and large-scale data processing. With over 1,000 computed nodes, equipped with two 12-core Intel Xeon Haswell CPUs and 128 GB of RAM, OKEANOS provides substantial computational power for advancing research in fields of engineering simulations.

The LS-PREPOST postprocessor was employed to facilitate detailed analysis and visualization of these results [19]. Displacement maps were presented using a colour scale, with warm colours indicating regions of high displacement and cold colours representing areas of low displacement. This allowed for the rapid identification of critical structural points. Additionally, the program enabled the examination of various stress tensor components, including principal, shear, and reduced stresses.

The calculations were performed across three variants, corresponding to three different vehicle speeds:

- $v = 15$  km/h (reconnaissance mode);
- $v = 25$  km/h (terrain traversability);
- $v = 50$  km/h (countryside);
- $v = 100$  km/h (maximal).

The figures below present only the critical components of the model that were directly subjected to numerical analysis using the finite element method. The focus is placed on key elements of the vehicle structure, such as the bumper, frame, and tree trunk, as these components play a key role in the collision simulation. Figure 7 illustrates the impact of the collision 5 ms after the vehicle bumper made contact with the tree trunk.

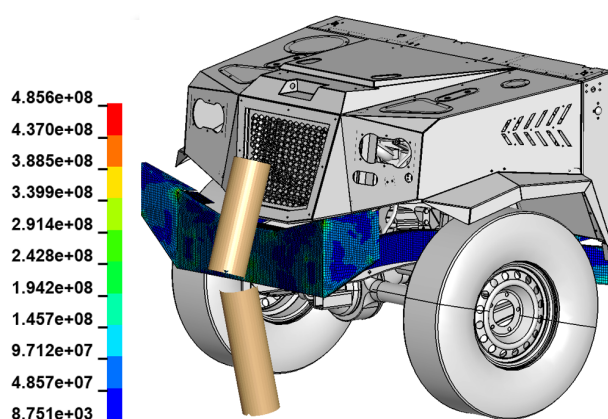


Fig. 6. HMH reduced stress map [Pa] for the following case:  
 $v = 25$  km/h,  $t = 30$  ms

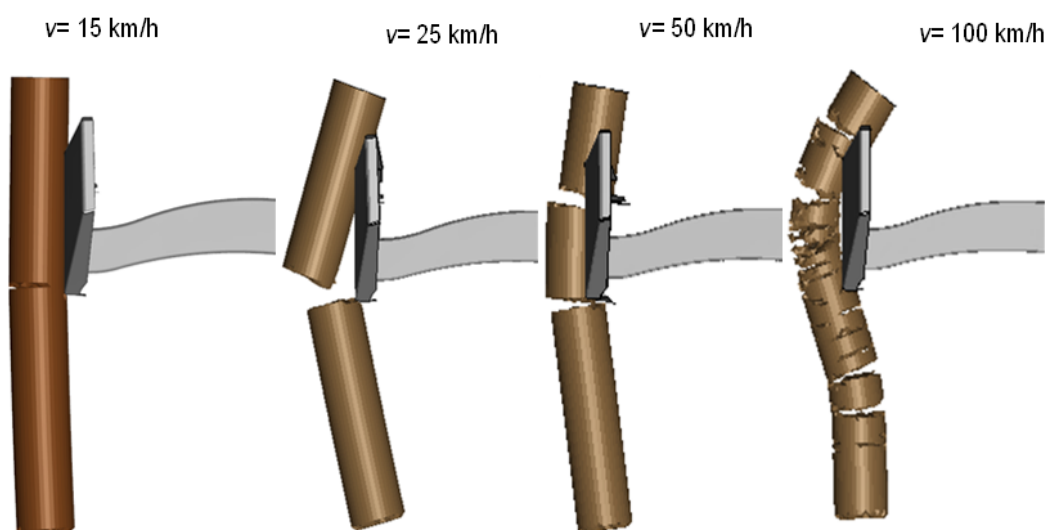


Fig. 7. Collision results 5 ms after the bumper starts to contact the trunk tree

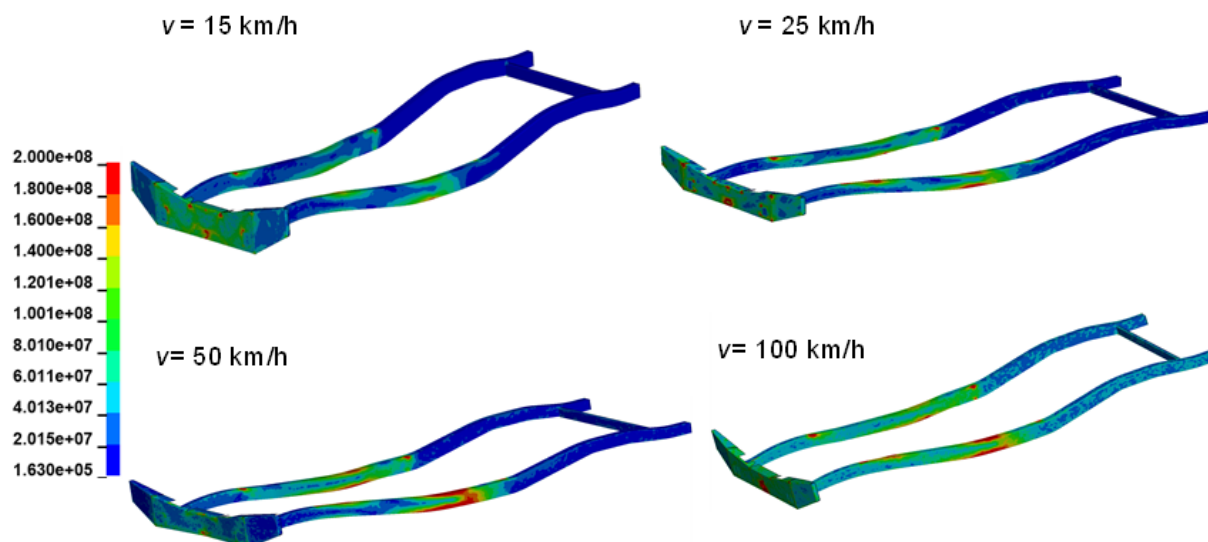


Fig. 8. HMM reduced stress of frame and bumper [Pa]

The analyzed variants considered various stages of the simulation: 6 ms, 30 ms, 15 ms, and 7.5 ms after the start of the vehicle's movement. This approach enables the capture of collision dynamics under varying conditions, allowing for an analysis of how varied factors influence the behaviour of the vehicle structure.

The reduced stresses, calculated according to the Huber-von Mises-Hencky hypothesis, in the bumper, side members, and cross members of the frame are presented in Fig. 8. The distribution of stresses clearly illustrates the role of the side parts during the collision, highlighting their contribution to energy absorption and structural deformation.

Minor damage, in the form of dents, can be observed in the bumper (Fig. 9). At higher speeds, a single noticeable dent appears, while at a speed of 25 km/h, the damage is almost imperceptible. This variation in damage severity highlights the influence of vehicle speed on the extent of deformation in the bumper during a collision.

The results of the conducted numerical simulations indicate that the impact of a typical obstacle in an unstructured terrain, such as a tree trunk, does not cause severe damage limiting

the vehicle's operational capability. There are only minor deformations observed during the simulations at higher speeds. These findings suggest that the vehicle design effectively absorbs impact energy, ensuring it remains operational even in challenging environments. The TAERO vehicle demonstrates sufficient structural integrity to withstand these impacts without compromising its functionality.

## 5. CONCLUSIONS

The study presents the preliminary evaluation of the structural resistance of the TAERO vehicle to typical obstacles encountered in unstructured terrains during special missions. The research focused on collision scenarios involving tree trunks, a common obstacle in unstructured terrains. Representative obstacle parameters were selected based on the characteristics of trees typical in Polish forests, ensuring the analyses represent operational conditions.

The study introduced an optimized numerical model for simulating vehicle collisions concentrated on the most influential

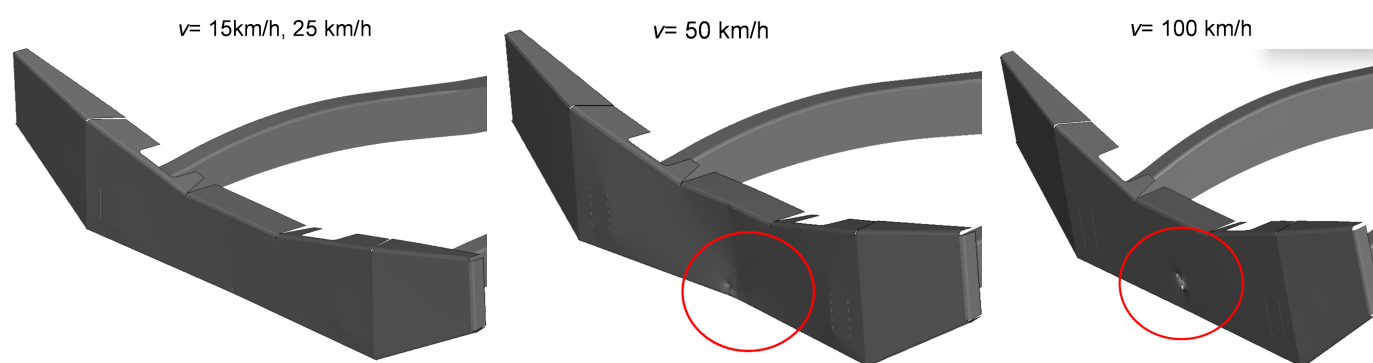


Fig. 9. Bumper dents after collision with analyzed trunk tree km/h,  $t = 30$  ms

structural elements. This approach effectively reduced computational demands while maintaining the accuracy required for the analyses conducted. The proposed model is a practical tool for quick vehicle performance evaluation.

The results confirmed that the TAERO vehicle meets strength requirements at all declared speeds, demonstrating its reliability for mission operations in challenging terrains. Structural validation remains important for its intended missions, where potential risks such as equipment damage or mission failure could lead to grave consequences.

Future research will investigate vehicle resistance to other types of obstacles commonly found in an unstructured environment validating performance and operational reliability.

## ACKNOWLEDGEMENTS

The research was conducted with the support of the Interdisciplinary Centre for Mathematical and Computational Modelling of the University of Warsaw (ICM UW). It is part of research project no. 55.23615.PR at the Military Institute of Armoured and Automotive Technology.

## REFERENCES

- [1] A. Gadekar *et al.*, “Recent developments in modular unmanned ground vehicles: A review,” *Asia-Pac. J. Sci. Technol.*, vol. 29, no. 01, p. 11, 2022.
- [2] J. Whitson, D. Gorsich, V. Vantsevich, and M. Letherwood, “Military Unmanned Ground Vehicle Maneuver: A Review and Formulation,” *SAE Tech. Paper*, 2023, doi: [10.4271/2023-01-0108](https://doi.org/10.4271/2023-01-0108).
- [3] T. Mikita *et al.*, “Mapping Forest Parameters to Model the Mobility of Terrain Vehicles,” *Forests*, vol. 15, no. 11, p. 1882, 2024, doi: [10.3390/f15111882](https://doi.org/10.3390/f15111882).
- [4] M. Nowakowski and J. Kurylo, “Usability of Perception Sensors to Determine the Obstacles of Unmanned Ground Vehicles Operating in Off-Road Environments,” *Appl. Sci.*, vol. 13, p. 4892, 2023, doi: [10.3390/app13084892](https://doi.org/10.3390/app13084892).
- [5] A.I. Kravcov, K. Civulová, O. Rolenec, M. Huber, P. Kubeček, and P. Simiński, “Proposal of Evaluation of Robotic Devices Trafficability, in Low-Endurable Terrain,” *Acta Polytech. Hung.*, vol. 21, no. 8, pp. 7–27, 2024.
- [6] R. Perz and M. Matyjewski, “Risk of Experiment Failure-Analysis of Crash Test Reliability,” *J. KONBiN*, vol. 29, no. 1, pp. 41–48, 2014.
- [7] B. Munyazikwiye, D. Vysochinskiy, K. Robbersmyr, and M. Khadyko, “Prediction of vehicle crashworthiness parameters using piecewise lumped parameters and finite element models,” *Designs*, vol. 2, no. 4, p. 43, 2018, doi: [10.3390/designs2040043](https://doi.org/10.3390/designs2040043).
- [8] P. Zmarzły, “Technological heredity of the turning process,” *Technicki Vjesnik*, vol. 27, no. 4, pp. 1194–1203, 2020, doi: [10.17559/TV-20190425150325](https://doi.org/10.17559/TV-20190425150325).
- [9] R. Grzejda, “Modeling the Normal Contact Characteristics between Components Joined in Multi-Bolted Systems,” *WSEAS Trans. Appl. Theor. Mech.*, vol. 19, pp. 73–81, 2024.
- [10] J. Hartwich, S. Sławski, and S. Duda, “Identification of nickel-titanium alloy material model parameters based on experimental research,” *J. Theor Appl Mech.*, vol. 62, no. 2, pp. 415–419, 2024, doi: [10.15632/jtam-pl/186510](https://doi.org/10.15632/jtam-pl/186510).
- [11] M. Chodnicki, M. Nowakowski, P. Pietruszewski, M. Wośowski, and S. Stępień, “BIZON–UGV for Airport Pavement Testing: Mechanics and Control,” *Appl. Sci.*, vol. 14, p. 2472, 2024, doi: [10.3390/app14062472](https://doi.org/10.3390/app14062472).
- [12] N. Korunović, “Structural optimization of an unmanned ground vehicle as part of a robotic grazing system design,” *Machines*, vol. 12, no. 5, p. 323, 2024, doi: [10.3390/machines12050323](https://doi.org/10.3390/machines12050323).
- [13] P. Sawczuk *et al.*, “Regeneration of the Damaged Parts with the Use of Metal Additive Manufacturing – Case Study,” *Materials*, vol. 16, p. 3772, 2023, doi: [10.3390/ma16103772](https://doi.org/10.3390/ma16103772).
- [14] M. Nowakowski, G.S. Berger, J. Braun, J.A. Mendes, L. Bonzatto, and J. Lima, “Advance Reconnaissance of UGV Path Planning Using Unmanned Aerial Vehicle to Carry Our Mission in Unknown Environment,” in *Robot 2023: Sixth Iberian Robotics Conference. ROBOT 2023. Lecture Notes in Networks and Systems*, vol. 978, L. Marques, C. Santos, J.L. Lima, D. Tardioli, and M. Ferre, Eds., Springer, Cham, 2024, doi: [10.1007/978-3-031-59167-9\\_5](https://doi.org/10.1007/978-3-031-59167-9_5).
- [15] P. Wysmulski, “Numerical and experimental study of crack propagation in the tensile composite plate with the open hole,” *Adv. Sci. Technol.-Res. J.*, vol. 17, no. 4, pp. 249–261, 2023.
- [16] LSTC, LS-DYNA. Theory manual. Livermore Software Technology Corporation. 2019.
- [17] J. Socha, L. Tymińska-Czabańska, K. Bronisz, S. Zięba, and P. Hawryło, “Regional height growth models for Scots pine in Poland,” *Sci. Rep.*, vol. 11, p. 10330, 2021, doi: [10.1038/s41598-021-89826-9](https://doi.org/10.1038/s41598-021-89826-9).
- [18] LSTC, LS-DYNA Manual vol. II R.13.0. Livermore Software Technology Corporation. 2021.
- [19] D. Aini *et al.*, “Introducing fatigue contour plot in LS-Pre Post LSDYNA finite element crash simulation software,” *Appl. Mech. Mater.*, vol. 165, pp. 275–279, 2012.